AGU PUBLICATIONS

JGR

Journal of Geophysical Research: Atmospheres

RESEARCH ARTICLE

10.1002/2014JD022116

Key Points:
- Heat flux events associated with polar vortex acceleration/deceleration
- Heat flux events associated with equatorward/poleward Atlantic jet shift
- Negative heat flux events play a key role during strong vortex events

Correspondence to:
E. Dunn-Sigouin,
ed2572@columbia.edu

Citation:
Dunn-Sigouin, E., and T. A. Shaw (2015), Comparing and contrasting extreme stratospheric events, including their coupling to the tropospheric circulation, *J. Geophys. Res. Atmos.*, *120*, 1374–1390, doi:10.1002/2014JD022116.

Received 2 JUN 2014
Accepted 26 JAN 2015
Accepted article online 29 JAN 2015
Published online 26 FEB 2015
Corrected 14 SEP 2015

This article was corrected on 14 SEP 2015. See the end of the full text for details.

Comparing and contrasting extreme stratospheric events, including their coupling to the tropospheric circulation

Etienne Dunn-Sigouin[1] and Tiffany A. Shaw[1,2]

[1]Department of Earth and Environmental Science, Lamont Doherty Earth Observatory, Columbia University, New York, USA, [2]Department of Applied Physics and Applied Math, Columbia University, New York, USA

Abstract Recent work has emphasized the importance of stratosphere-troposphere coupling associated with extreme values of the polar vortex strength and stratospheric planetary wave heat flux during Northern Hemisphere winter. Here using ERA-Interim reanalysis data the evolution of the two types of events are compared. The life cycle of total (anomaly plus climatology) positive/negative heat flux events are associated with vertically deep high-latitude planetary wave structures and exhibit largely equal but opposite-signed impacts, including a net deceleration/acceleration of the polar vortex due to EP flux convergence/divergence and an equatorward/poleward tropospheric jet shift in the North Atlantic. The tropospheric wave pattern is westward propagating. High-latitude stratospheric vertical zonal wind shear plays a key role during both events. A comparison of the stratospheric events reveals that planetary wave events contribute to the development of vortex events. In particular, total negative heat flux events precede strong vortex events showing that strong vortex events represent true dynamical events involving significant wave-mean flow interaction. Coupling with the North Atlantic jet occurs preceding vortex events when wave-1 dominates the total eddy heat flux in the lower stratosphere since interference with wave-2 makes the impacts less clear. The tropospheric impacts in the North Atlantic associated with planetary wave events are found to be comparable if not larger than those following vortex events.

1. Introduction

It is well established that variability of the wintertime stratospheric polar vortex is coupled to anomalous weather regimes in the troposphere. This variability is often characterized by weak and strong polar vortex events defined as extreme values of the stratospheric Northern Annular Mode (NAM) [e.g., *Baldwin and Dunkerton*, 2001; *McLandress and Shepherd*, 2009; *Gerber et al.*, 2010; *Hitchcock et al.*, 2013]. Weak vortex events, which are associated with Stratospheric Sudden Warmings (SSWs), involve downward migrating negative zonal-mean zonal wind anomalies and an equatorward shift of the zonal-mean tropospheric jet for several weeks following the event [*Baldwin and Dunkerton*, 2001; *Limpasuvan et al.*, 2004]. Conversely, strong vortex events involve downward migrating positive zonal-mean zonal wind anomalies and a poleward shift of the zonal-mean tropospheric jet [*Baldwin and Dunkerton*, 2001; *Limpasuvan et al.*, 2005].

Another fundamental source of vertical coupling between the stratosphere and the troposphere is planetary-scale waves [*Plumb*, 2010]. Planetary waves are primarily generated in the troposphere and couple vertically with the stratosphere when the mean flow is westerly [*Charney and Drazin*, 1961; *Matsuno*, 1970]. *Perlwitz and Harnik* [2003] showed that the time scale of vertical wave coupling is on the order of 5 days between 500 and 10 hPa. Vertical wave coupling can be characterized by the vertical component of the Eliassen-Palm (EP) flux, which is proportional to the meridional heat flux and connected to the wave vertical group velocity according to linear theory.

Recent research has revealed that the wintertime distribution of high-latitude planetary wave heat flux exhibits extreme values that are linked to the tropospheric circulation in the North Atlantic. *Shaw and Perlwitz* [2013] analyzed total (anomaly plus climatology) negative wave-1 heat flux values, which represent extremes of the wintertime distribution. The event life cycle occurred over two weeks and involved vertical coupling via a high-latitude wave-1 signal. The high-latitude signal in the troposphere produces circulation anomalies that resemble the positive phase of the North-Atlantic Oscillation (NAO), including a poleward jet shift over the North Atlantic. A subsequent study by *Shaw et al.* [2014] showed that extreme positive and negative stratospheric wave-1 heat flux values are instantaneously linked to tropospheric patterns resembling opposite phases of the NAO. Finally, *Shaw and Perlwitz* [2014] showed that extreme negative

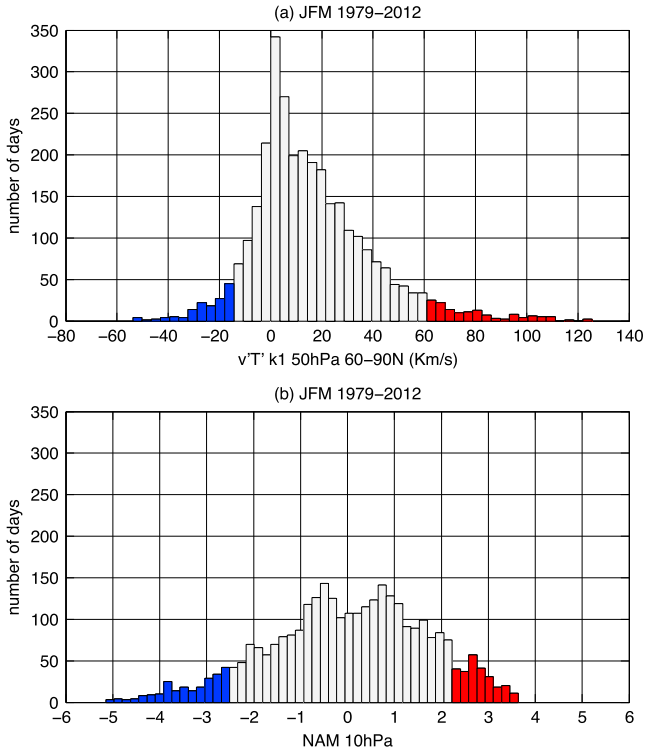

Figure 1. (a) Histogram of the daily wave-1 meridional heat flux averaged from 60 to 90°N at 50 hPa during JFM for 1979–2012. (b) Histogram of the daily NAM index at 10 hPa during JFM for 1979–2012. Blue and red shading denote the amplitude thresholds used to define extreme stratospheric events (see section 2 for details).

stratospheric heat flux values are associated with divergence of Eliassen-Palm flux and a reversal of the residual circulation in the Arctic stratosphere.

Previous research has linked anomalous time-integrated heat flux variability at 100 hPa to zonal-mean stratospheric variability in the Arctic. *Newman et al.* [2001] showed that the time-integrated anomalous 45 to 75°N heat flux during January and February is correlated with extreme Arctic temperatures during March. *Polvani and Waugh* [2004] showed that weak/strong vortex events are preceded by anomalous 40 day time-integrated positive/negative heat fluxes at 100 hPa. The results suggest that anomalous time-integrated heat flux values are important for the zonal-mean flow. However, an anomalous time-integrated heat flux does not provide a clear physical interpretation. It could reflect a single positive heat flux event or a prolonged strong positive event. Similarly, an anomalous negative heat flux event could imply a weakened climatology or a total negative heat flux. Thus, it is unclear what the role of individual heat flux events are during the life cycle of vortex events.

Our goal here is to better understand the connections between extreme stratospheric heat flux and polar vortex events, including their coupling to the tropospheric circulation. We define upward/downward planetary wave events as extreme positive/negative values of the total wave-1 high-latitude stratospheric heat flux, consistent with the connection between the sign of the heat flux and the vertical group velocity. We define weak/strong vortex events as extreme negative/positive values of the stratospheric NAM following previous research. We analyze the life cycle of the events in reanalysis data and seek to answer the following questions:

1. What are the stratospheric and tropospheric impacts associated with the transient evolution of planetary wave events? Previous studies have documented instantaneous impacts of extreme stratospheric heat fluxes and the life cycle of negative heat flux events [*Shaw and Perlwitz*, 2013, 2014; *Shaw et al.*, 2014]. The evolution of positive heat flux events has not been documented.
2. What role does the zonal-mean flow play in the transient evolution of planetary wave events? *McIntyre* [1982] suggests that a strengthened and contracted polar vortex is important for "focusing" anomalous upward propagating waves into high latitudes where they can produce large impacts on the zonal-mean flow. Previous studies have also highlighted the importance of high-latitude vertical zonal-mean zonal wind shear [*Perlwitz and Harnik*, 2003, 2004; *Shaw et al.*, 2010; *Shaw and Perlwitz*, 2013].
3. Do planetary wave events play a role during polar vortex events? We seek a clear physical interpretation of the connection between anomalous time-integrated heat flux and vortex events documented by *Polvani and Waugh* [2004].
4. Finally, how do the tropospheric impacts during planetary wave and polar vortex events compare in the North Atlantic? Much of the recent work on stratosphere-troposphere coupling has focused on the impact of vortex events, particularly SSWs. The recent study by *Shaw et al.* [2014] showed that planetary wave

Table 1. Central dates of upward and downward wave-1 and wave-2 events and weak and strong vortex events.

Upward Wave 1	Downward Wave 1	Upward Wave 2	Downward Wave 2	Weak Vortex	Strong Vortex
25 Jan 1979	1 Mar 1979	22 Feb 1979	8 Feb 1979	23 Feb 1979*	—
—	—	—	10 Mar 1979	—	—
—	—	—	26 Mar 1979	—	—
25 Jan 1980	—	14 Feb 1980	4 Feb 1980	—	6 Feb 1980
26 Feb 1980	—	—	6 Mar 1980	—	—
31 Jan 1981	17 Feb 1981	—	—	4 Feb 1981	—
7 Jan 1982	14 Mar 1982	20 Jan 1982	17 Feb 1982	24 Jan 1982	—
—	—	12 Mar 1982	5 Mar 1982	—	—
21 Feb 1983	—	29 Jan 1983	—	—	—
23 Feb 1984	10 Feb 1984	13 Jan 1984	—	25 Feb 1984*	24 Jan 1984
—	—	12 Mar 1984	—	—	—
–	25 Jan 1986	15 Feb 1986	—	—	25 Feb 1986
–	26 Mar 1986	22 Mar 1986	—	—	—
—	—	—	—	19 Jan 1987*	—
10 Mar 1988	—	25 Feb 1988	—	—	25 Jan 1988
—	27 Feb 1989	6 Feb 1989	—	19 Feb 1989*	14 Jan 1989
7 Feb 1990	14 Feb 1990	20 Feb 1990	29 Jan 1990	—	11 Mar 1990
—	23 Mar 1990	—	14 Feb 1990	—	—
—	—	—	31 Mar 1990	—	—
2 Jan 1991	1 Feb 1991	2 Feb 1991	13 Jan 1991	—	—
—	—	—	10 Feb 1991	—	—
12 Jan 1992	23 Jan 1992	—	—	14 Jan 1992	—
4 Mar 1993	22 Mar 1993	16 Mar 1993	5 Feb 1993	—	20 Jan 1993
—	11 Mar 1994	4 Feb 1994	7 Jan 1994	1 Jan 1994	27 Feb 1994
—	—	—	24 Feb 1994	—	—
—	—	—	14 Mar 1994	—	—
21 Jan 1995	14 Feb 1995	—	23 Mar 1995	2 Feb 1995	9 Mar 1995
—	29 Mar 1995	—	—	—	—
14 Feb 1996	13 Jan 1996	11 Mar 1996	2 Jan 1996	—	6 Feb 1996
1 Mar 1996	14 Mar 1996	—	12 Feb 1996	—	—
—	—	—	3 Mar 1996	—	—
—	—	—	22 Mar 1996	—	—
—	28 Feb 1997	—	9 Feb 1997	—	—
1 Feb 1998	—	—	—	—	—
23 Feb 1999	—	—	—	26 Feb 1999*	—
—	11 Feb 2000	15 Jan 2000	—	—	9 Jan 2000
—	23 Mar 2000	18 Mar 2000	—	—	29 Jan 2000
—	—	—	—	—	24 Feb 2000
—	—	—	—	9 Feb 2001*	—
—	8 Mar 2002	—	6 Jan 2002	—	—
14 Jan 2003	—	—	10 Jan 2003	17 Jan 2003*	—
—	—	—	6 Feb 2003	—	—
—	—	—	25 Feb 2003	—	—
—	—	—	31 Mar 2003	—	—
—	—	—	—	1 Jan 2004*	—
26 Feb 2005	8 Feb 2005	—	—	14 Mar 2005	15 Jan 2005
13 Mar 2005	—	—	—	—	8 Feb 2005
—	—	—	24 Jan 2006	13 Jan 2006*	—
24 Feb 2007	10 Jan 2007	—	1 Jan 2007	—	—
—	—	—	5 Mar 2007	—	—
20 Feb 2008	28 Jan 2008	—	18 Jan 2008	23 Feb 2008*	—
—	28 Feb 2008	—	18 Feb 2008	—	—
—	—	—	18 Mar 2008	—	—
—	—	19 Jan 2009	—	23 Jan 2009*	6 Jan 2009

Table I. (Continued)

Upward Wave 1	Downward Wave 1	Upward Wave 2	Downward Wave 2	Weak Vortex	Strong Vortex
25 Jan 2010	—	—	—	—	—
7 Jan 2011	—	1 Feb 2011	20 Jan 2011	—	6 Mar 2011
—	—	23 Mar 2011	6 Feb 2011	—	—
—	—	—	5 Mar 2011	—	—
14 Jan 2012	26 Jan 2012	—	8 Feb 2012	—	—
25	26	21	37	17	17

*Asterisks denote weak vortex dates within 10 days of stratospheric sudden warmings according to [*Hitchcock et al.*, 2013].

coupling produces large regional impacts in the North Atlantic. It is important to understand what indices should be monitored in order to forecast tropospheric impacts of extreme stratospheric events.

This paper is organized as follows. Section 2 describes the data and methods. Section 3.1 shows the composite life cycle of upward and downward planetary wave events. In section 3.2, we illustrate the connections between planetary wave and polar vortex events. Section 3.3 compares the life cycle of vortex and planetary wave events, including their tropospheric impacts. Our conclusions are summarized and discussed in section 4.

2. Data and Methods

2.1. Data

This study is based on 34 years of three-dimensional daily January, February, and March (JFM) data from the European Centre for Medium-Range Weather forecasts Interim (ERA-Interim) reanalysis data set [*Dee et al.*, 2011] from 1979 to 2012. We focus our analysis during JFM which is the time period of maximum planetary wave coupling in the Northern Hemisphere [*Shaw et al.*, 2010]. Qualitatively similar results are found using the extended NDJFM winter season (not shown). Here anomalies are defined as deviations from the daily climatological annual cycle calculated from the entire record and statistical significance is reported at the 95% level based on a two-tailed students *t*-test. A 5 day running mean is applied to all data. The results are not sensitive to the length and type of smoothing (not shown) consistent with the fact that the results are in good agreement with *Shaw and Perlwitz* [2013] and *Shaw et al.* [2014] who use a 5 day smoothing and no smoothing, respectively.

2.2. Planetary Wave Events

In our analysis, we define planetary wave events using the daily zonal-mean wave-1 meridional heat flux, i.e., $\overline{v'T'}_{k=1}$, where v and T are meridional wind and temperature, primes denote deviations from the zonal-mean, and $k = 1$ denotes zonal wavenumber 1. The 50 hPa wave-1 heat flux is weighted by the cosine of latitude and meridionally averaged from 60 to 90°N producing a daily JFM time series for the entire record ($34 \times 90 = 3060$ days). Hereafter, we define this quantity as the high-latitude heat flux. Recall that the zonal-mean meridional heat flux is related to the vertical component of the EP flux, which according to linear theory is proportional to the vertical group velocity and is thus a measure of vertical wave propagation. We focus on wave-1 because it dominates the total eddy (deviation from zonal-mean) heat flux in the stratosphere and use a high-latitude average because the leading empirical orthogonal function of the wave-1 heat flux peaks over the polar cap [*Shaw and Perlwitz*, 2013]. The results are not sensitive to the choice of stratospheric pressure level (e.g., 30 or 70 hPa), latitudinal average (e.g., 45 to 75°N) or the choice of vertical EP flux instead of eddy heat flux.

Figure 1a shows the daily high-latitude wave-1 heat flux distribution at 50 hPa. The high-latitude heat flux exhibits significant variability in the stratosphere. The mean value is +16 Kms^{-1}, reflecting a Northern Hemisphere winter climatology dominated by upward wave propagation. The 22nd percentile of the distribution is approximately 0 Kms^{-1}, indicating that a significant number of days correspond to downward wave propagation according to linear theory. As such, the percentile of the zero heat flux provides a physically based measure of extreme heat flux values. The high-latitude wave-2 heat flux distribution at

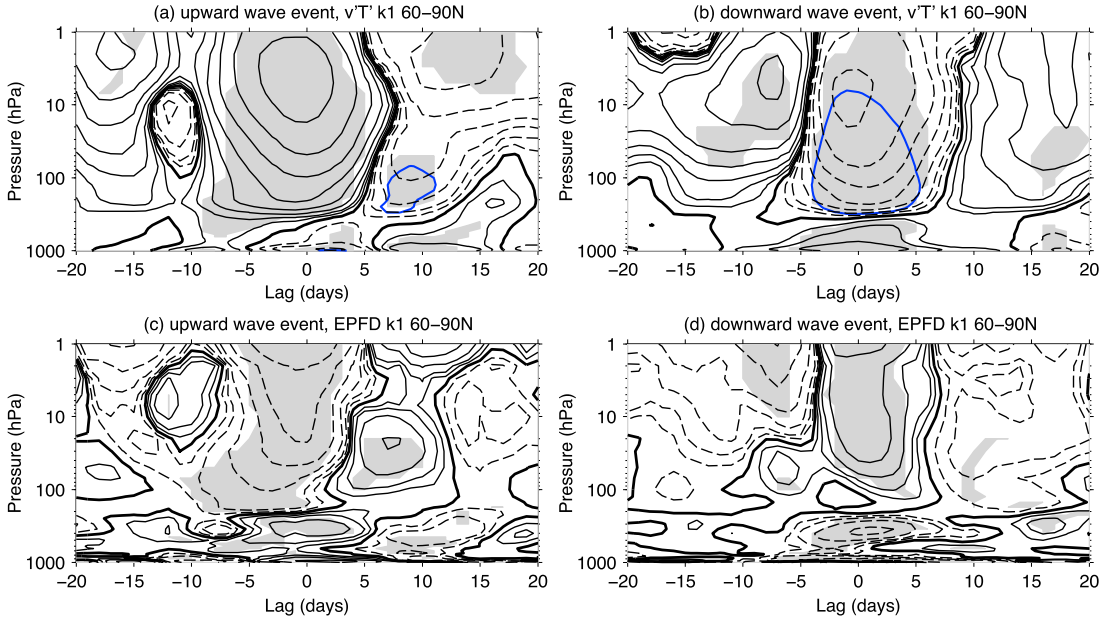

Figure 2. Evolution of the (a, c) upward and (b, d) downward planetary wave events as a function of time from days −20 to +20 and pressure: (a, b) wave-1 meridional heat flux anomaly (black contours) and zero contour of the total wave-1 meridional heat flux (blue contour) averaged 60 to 90°N. (c, d) Wave-1 EP flux divergence anomaly averaged 60 to 90°N. The black contour intervals are logarithmic powers of 2: ± [1, 2, 4 ,8, 16, 32, ...] Kms^{-1} and ± [0.5, 1, 2, 4 , 8, 16, ...] $ms^{-1}day^{-1}$ for Figures 2a and 2b and Figures 2c and 2d, respectively. Dashed lines are negative, and the thick black line is the zero contour. Shading indicates statistical significance at the 95% level based on a two-tailed *t*-test.

50 hPa exhibits smaller mean and extreme values consistent with its smaller contribution to the total eddy heat flux (see Figure A2).

The composite life cycle of planetary wave events is based on the daily high-latitude heat flux time series. An upward/downward planetary wave event is identified when the time series first crosses the 95th/5th percentile of the JFM distribution, corresponding to a value of +59.3/−13.5 Kms^{-1} denoted with red/blue shading in Figure 1a. The central date (day 0) is defined as the day of maximum or minimum heat flux. Finally, the central dates of each type of event must be separated by at least 15 days. The time separation threshold is motivated by the time scale of planetary wave coupling [*Perlwitz and Harnik*, 2003]. Using these criteria, we identify 25 upward and 26 downward wave events during 34 JFM seasons from 1979 to 2012 (see Table I). It should be noted that 4 of the 26 downward wave events are preceded by upward wave events within 15 days, indicating that the upward and downward wave events occur relatively independently. Qualitatively similar results are obtained for different choices of the central date, amplitude or time separation threshold. For completeness, important aspects of the composite life cycle of upward and downward wave-2 events, defined using the high-latitude wave-2 heat flux time series, are shown in the appendix.

Our definition of downward planetary wave events is slightly different than the definition of *Shaw and Perlwitz* [2013] who used the principal component time series of the wave-1 heat flux at 30 hPa. However our results are qualitatively similar overall. We note that 12 of their 14 events occur within 10 days of the downward planetary wave events defined here (Table I).

2.3. Polar Vortex Events

Polar vortex events are defined using the daily JFM time series of the 10 hPa NAM defined as the normalized principal component of the leading empirical orthogonal function of zonal-mean geopotential height anomalies from 0 to 90°N consistent with previous research [e.g., *Baldwin and Dunkerton*, 2001; *Baldwin and Thompson*, 2009]. Hereafter, we define this as the NAM index. The NAM index is a well-known measure of the polar vortex strength. Figure 1b shows the daily NAM distribution at 10 hPa.

The composite life cycle of vortex events is based on the daily NAM index time series. The central date (day 0) of a weak/strong vortex event is defined as the day when the NAM time series first crosses −2.5/ +

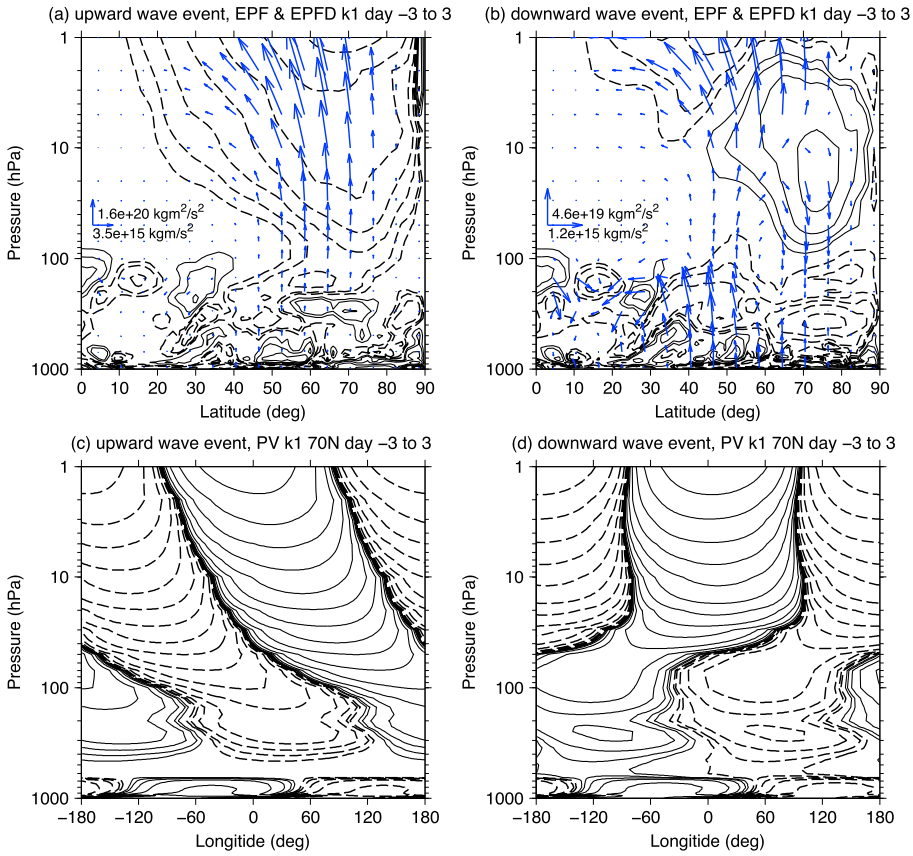

Figure 3. (a, b) Total wave-1 EP flux (vectors) and EP flux divergence (contours) as a function of latitude and pressure and (c, d) wave-1 potential vorticity at 70°N as a function of longitude and pressure during days −3 to +3 of (a, c) upward and (b, d) downward planetary wave events. The contour intervals are logarithmic powers of 2: ± [0.5, 1, 2, 4 ,8, 16, ...] $ms^{-1}day^{-1}$ and ± [0.0625, 0.125, 0.25, 0.5, 1, 2, ...] *PVU* for Figures 3a and 3b and Figures 3c and 3d, respectively. Dashed lines are negative. The EP flux vectors are scaled as in *Dunkerton et al.* [1981] and multiplied by $e^{z/H}$, where *H* is the scale height.

2.25 standard deviations, denoted with blue/red shading in Figure 1b. In addition, the central dates of each event must be separated by at least 20 days and we require that the NAM time series rise above/drops below the event threshold 40 days following the central date. Using these criteria, 17 weak and 17 strong vortex events are identified during 34 JFM seasons from 1979 to 2012 (see Table I). Note that our definition of weak vortex events does not separate different types of SSWs (e.g., major, minor, split, and displacement). For reference, 14 (11) of our 17 weak vortex events occur within 10 days of the weak vortex (SSW) events listed in *Hitchcock et al.* [2013] (see their Figure 12 and Table 1). Our weak vortex central dates differ from those in *Limpasuvan et al.* [2004] most likely due to differences in the central date definition. However, when we synchronize the stratospheric evolution of our events as in *Limpasuvan et al.* [2004], we find good agreement with their results. The central dates of the strong vortex events compare well with *Limpasuvan et al.* [2005]. Finally, qualitatively similar results are obtained for different choices of the central date, amplitude or time separation thresholds.

3. Results

3.1. The Life Cycle of Planetary Wave Events

The composite life cycle of upward and downward planetary wave events are shown in Figures 2–5 (left and right, respectively). Figure 2 shows the evolution of the high-latitude wave-1 heat flux anomaly (a, b) and high-latitude wave-1 EPFD anomaly (c, d) as a function of pressure and time from −20 to +20 days. The EP fluxes are computed for the primitive equations in log-pressure coordinates [see *Andrews et al.*, 1987] [Wave-2 heat fluxes are weak in the stratosphere during the composite life cycles (not shown)].

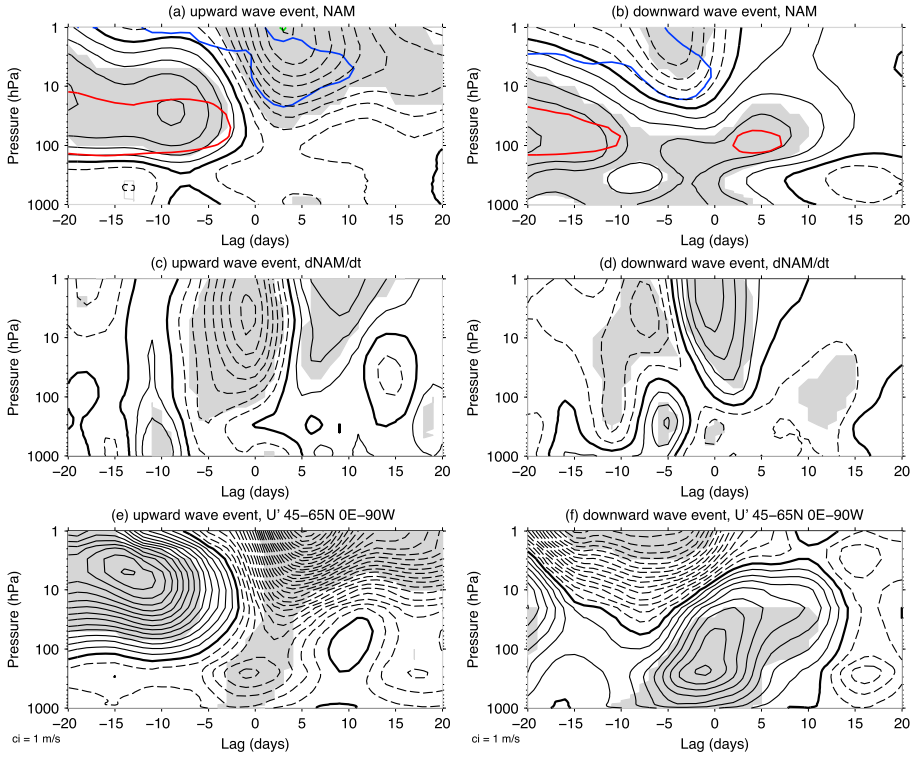

Figure 4. Evolution of the (a, c, e) upward and (b, d, f) downward planetary wave events as a function of time from days −20 to +20 and pressure. (a, b) NAM index (black contours), zero contour of the zonal-mean zonal wind averaged 60 to 80°N (green contour) and positive and negative vertical zonal wind shear above 200 hPa averaged 60 to 80°N (red and blue contours). The black contour interval is 0.25; blue and red contours denote the $-4 \times 10^{-4}\ s^{-1}$ and $12 \times 10^{-4}\ s^{-1}$ contours, respectively. (c, d) NAM time-tendency with a contour interval of 0.05 day^{-1}. (e, f) Zonal wind anomalies averaged 45 to 65°N and 90°W to 0°E with a contour interval of 1 ms^{-1}. Dashed lines are negative and the thick black line is the zero contour. Shading indicates statistical significance at the 95% level based on a two-tailed *t*-test.

During the upward planetary wave event, there is a positive heat flux anomaly that migrates from the troposphere to the upper stratosphere from days −10 to −5 (Figure 2a). It is difficult to establish a vertical propagation time scale because the coupling is nearly instantaneous in high latitudes. However, the evolution of the vertical EP flux averaged 45–90°N shows a clear low-latitude tropospheric precursor followed by upward propagation into the high-latitude stratosphere on the order of 6 days (not shown). The maximum heat flux anomaly in the stratosphere occurs between days −5 to +5 with significant negative heat flux anomalies in the troposphere. The vertical heat flux anomaly dipole subsequently changes sign from days +5 to +15 producing negative wave-1 heat flux anomalies in the stratosphere. The heat flux anomaly in the lower stratosphere represents a total negative wave-1 heat flux (blue contour), suggesting downward wave propagation.

The heat flux evolution coincides with large changes in anomalous wave-1 EPFD in high latitudes (Figure 2c). The heat flux anomaly coincides with a vertical EPF convergence/divergence anomaly dipole in the stratosphere/troposphere during the event that changes sign on day +5 producing a EPF divergence/convergence dipole. The high-latitude wave-1 EPFD is dominated by the vertical component from days −10 to +15 (not shown).

During the downward planetary wave event, the high-latitude heat flux anomaly exhibits similar behavior but with different timing and a dominant negative heat flux pulse (Figure 2b). In particular, the event begins with a positive high-latitude stratospheric heat flux anomaly from days −15 to −5. Note that the positive heat flux anomaly is both weaker in magnitude and shorter in duration than the pulse during the upward wave event. The stratospheric heat flux anomaly subsequently changes sign and reaches its minimum value between days −5 to +5 and is coupled to significant positive tropospheric heat flux anomalies. The evolution of the heat flux anomalies is consistent with the results of *Shaw and Perlwitz* [2013] (see their Figure 2).

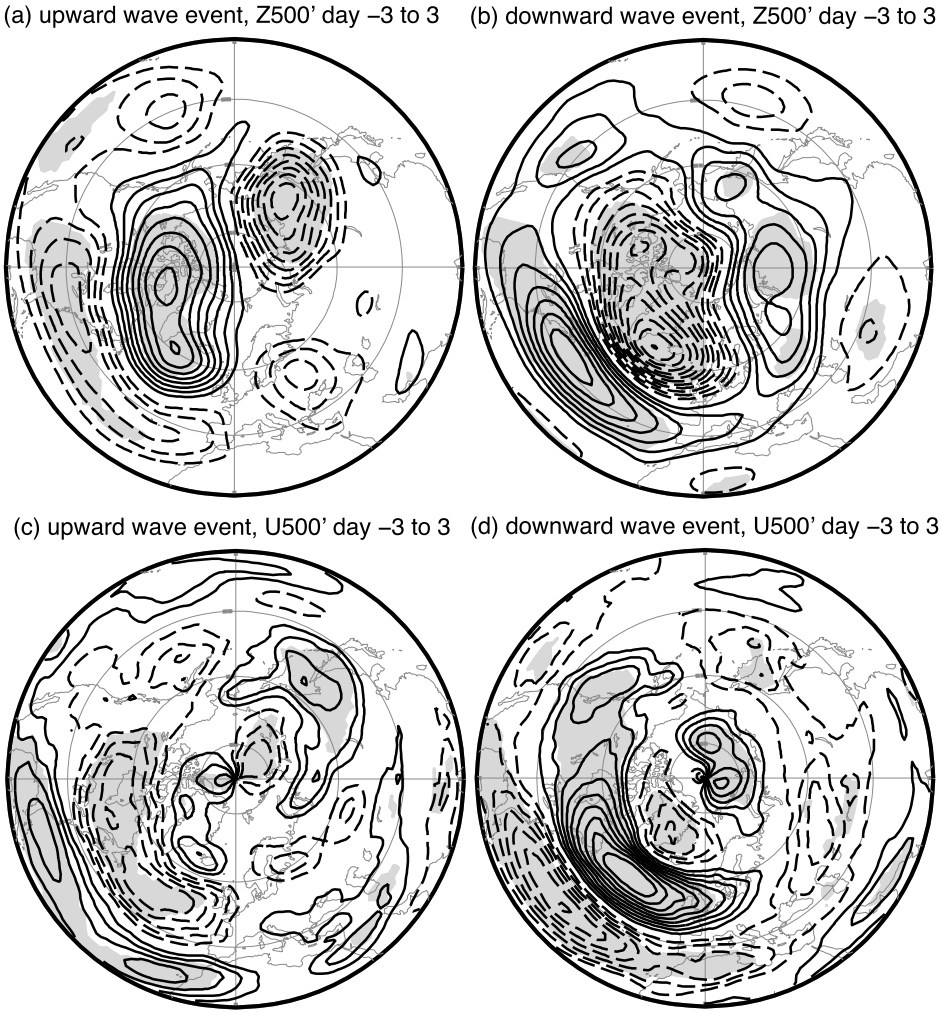

Figure 5. (a, b) Geopotential height anomalies and (c, d) zonal wind anomalies at 500 hPa during days −3 to +3 of (a, c) upward and (b, d) downward planetary wave events. Dashed lines are negative and the contour interval is 10 *m* and 1 ms^{-1} for Figures 5a and 5b and Figures 5c and 5d respectively. Shading indicates statistical significance at the 95% level based on a two-tailed *t*-test.

The high-latitude heat flux evolution coincides with vertical dipoles of EPF divergence/convergence anomalies in the stratosphere/troposphere (Figure 2d). The high-latitude wave-1 EPFD is dominated by the vertical component (not shown).

The high-latitude vertical dipole of anomalous wave-1 EPFD during extreme planetary wave events is consistent with transient wave propagation. In particular, the upward pointing total wave-1 EP flux vectors and EPFD convergence/divergence dipole in high latitudes during the upward wave event are suggestive of upward wave propagation from the tropospheric source to the stratospheric sink (Figure 3a). This interpretation is consistent with the westward phase tilt with height of the wave-1 potential vorticity at 70°N during days −3 to +3 (Figure 3c). We note however that the short time scales and meridional averaging involved make it difficult to determine a propagation time scale. The meridional component of the EPF vectors indicate propagation and convergence into the high-latitude upper stratosphere. Similarly, the downward pointing total wave-1 EP flux vectors and opposite-signed EPFD dipole in high latitudes during the downward wave event are consistent with transient downward wave propagation from the stratosphere to the troposphere (Figure 3b). This interpretation is consistent with the vertical standing wave-1 pattern at 70°N during days −3 to +3, which suggests interference between upward and downward wave propagation (Figure 3d). The meridional component of the EPF vectors also suggest propagation into high latitudes and subsequent vertical divergence.

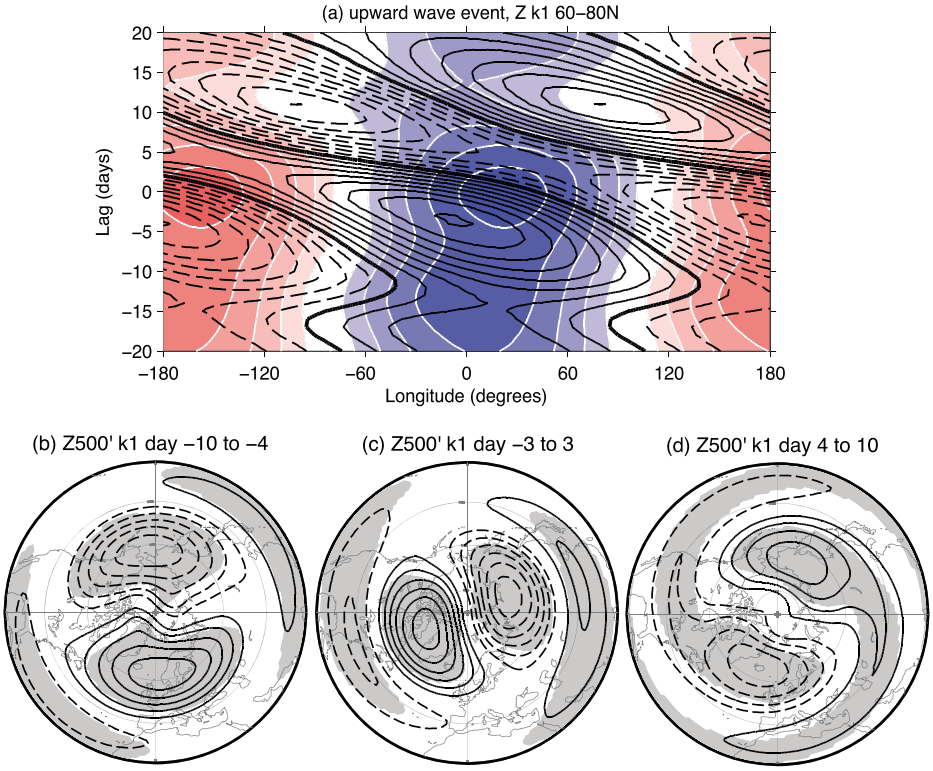

Figure 6. (a) Evolution of zonal wave-1 geopotential height averaged from 60 to 80°N at 10 hPa (color shading) and 500 hPa (black contours) for the upward planetary wave event as a function of time from −20 to +20 days and longitude. Contour interval is 200 m (color shading) and 10 m (black contours). (b, c, d) Zonal wave-1 geopotential height anomalies at 500 hPa averaged over days −10 to −4, −3 to +3, and +4 to +10. Contour interval is 10 m. Shading indicates statistical significance at the 95% level based on a two-tailed *t*-test.

The corresponding transient evolution of the zonal-mean flow, including the NAM, NAM time-tendency, and anomalous zonal wind in the North Atlantic (45 − 65°N 90°W − 0°E) (top, middle, and bottom, respectively) during upward (left) and downward (right) planetary wave events is shown in Figure 4. We focus on the tropospheric impacts in the North Atlantic because *Shaw et al.* [2014] documented clear links between that region and extreme stratospheric heat fluxes. During the upward wave event, the NAM transitions from a large positive value in the lower stratosphere to a large negative value in the upper stratosphere around day −5 (Figure 4a). While the NAM values are large and statistically significant they do not represent extreme values of the NAM index. The time evolution is associated with a large negative NAM time-tendency around day 0 and a subsequent positive tendency afterward (Figure 4c) which is consistent with the evolution of the high-latitude EPFD anomalies (Figure 2c). The large negative EPFD anomalies in the stratosphere between days −10 to +4 produce an anomalous deceleration of the polar vortex and the subsequent positive EPFD anomalies between days +4 to +12 produce an anomalous acceleration of the polar vortex. Since the upward wave event is transient and involves positive and negative dipoles, it is possible that the effects could integrate to zero over their life cycles meaning the impacts would be reversible. However, the time-integrated NAM tendency and the EPFD are negative indicating an irreversible deceleration of the polar vortex.

The life cycle of the downward wave event reveals similar connections between the NAM, NAM tendency, and the high-latitude EPFD anomalies (Figures 4b and 4d). In particular, negative EPFD anomalies in the stratosphere produce a weakening of the polar vortex and thus a negative NAM tendency which is followed by a period of large positive EPFD and positive NAM tendency producing a strengthening of the polar vortex (Figure 2d). Note that the time-integrated NAM tendency and EPFD are positive indicating a net acceleration of the polar vortex. The evolution is consistent with the dynamical acceleration in high latitudes during the "sudden stratospheric cooling" event reported by *Palmer and Hsu* [1983]. Such cooling events were shown to occur during days with negative stratospheric heat flux and involve a reversal of the residual circulation [*Shaw and Perlwitz*, 2014].

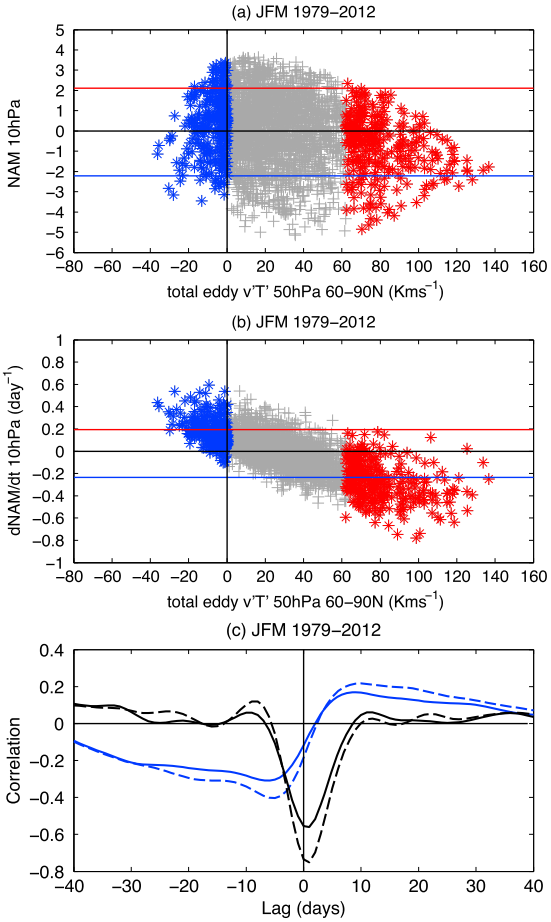

Figure 7. (a) Scatter plot of the daily total eddy meridional heat flux at 50 hPa averaged 60 to 90°N versus the NAM at 10 hPa. Blue and red stars/lines denote the 14th and 86th percentile days of the total eddy meridional heat flux at 50 hPa/NAM at 10 hPa during JFM (see text for details). (b) Same as above except for the total eddy meridional heat flux at 50 hPa averaged 60 to 90°N versus the NAM time-tendency at 10 hPa. (c) Lag correlation of total eddy meridional heat flux at 50 hPa averaged 60 to 90°N and NAM at 10 hPa (blue dashed), of zonal wave-1 meridional heat flux at 50 hPa averaged 60 to 90°N and NAM at 10 hPa (blue solid), of total eddy meridional heat flux at 50 hPa averaged 60 to 90°N and NAM time-tendency at 10 hPa (black dashed) and of zonal wave-1 meridional heat flux at 50 hPa averaged 60 to 90°N and NAM time-tendency at 10 hPa (black solid). For all panels, the black lines denote the zero lines.

The results suggest strong coupling between the wave and zonal-mean flow during the life cycle of planetary wave events. Recall that a strengthened and contracted polar vortex, associated with large positive vertical zonal wind shear, is conducive to wave focusing into the high-latitude stratosphere consistent with enhanced positive heat fluxes [*McIntyre*, 1982]. Conversely, a negative vertical zonal wind shear (vertical reflecting surface) corresponds to planetary wave reflection in high-latitudes and total negative stratospheric heat fluxes [*Perlwitz and Harnik*, 2003, 2004; *Shaw et al.*, 2010; *Shaw and Perlwitz*, 2013]. The life cycle of planetary wave events involve large transient changes in the stratospheric vertical zonal-mean zonal wind shear (red and blue contours) and a reversal of the zonal-mean zonal wind (green contour) averaged from 60 − 80°N (Figures 4a and 4b). During the upward planetary wave event, there is strong positive lower stratospheric vertical zonal wind shear from days −20 to −5, indicating the polar vortex is focused in high latitudes (not shown). This is followed by a reversal of the zonal-mean zonal wind in the upper stratosphere from days +3 to +4 and a period of strong negative vertical zonal wind shear near 10 hPa from days 0 to +10. The period of negative vertical zonal wind shear coincides with total negative heat fluxes in the lower stratosphere consistent with a wave in the presence of a vertically reflecting surface (Figure 2b). The life cycle of the downward planetary wave event also involves large negative vertical zonal wind shear in the stratosphere prior to the negative heat flux minimum (compare Figures 2b and 4b).

During the planetary wave events, the largest coupling with the tropospheric circulation occurs in the North Atlantic (Figures 4e and 4f). During the upward wave event, there is significant negative North Atlantic zonal wind anomalies in the troposphere between days −5 to +5 (compare Figure 4e with Figure 2a). Similarly, the downward wave event coincides with significant positive North Atlantic zonal wind anomalies between days −5 to +5. Note that the North Atlantic zonal wind anomalies dominate the time-integrated life cycle for both planetary wave events and produce a zonal-mean jet shift. In the zonal mean, the jet shift is consistent with anomalous convergence/divergence of wave-1 meridional EPFD during upward/downward wave events (not shown).

Figures 5a and 5b illustrate the links between planetary wave events and the tropospheric circulation during the period of maximum North Atlantic zonal wind anomalies in the troposphere (days −3 to +3). The 500 hPa geopotential height anomalies have a distinct wave-1 structure in high latitudes. The spatial structure of the geopotential height anomalies in the North Atlantic is reminiscent of opposite phases of the NAO. This is further illustrated in the composite 500 hPa zonal wind anomalies (Figures 5c and 5d), which show a clear equatorward/poleward jet shift in the North Atlantic during the upward/downward planetary wave events.

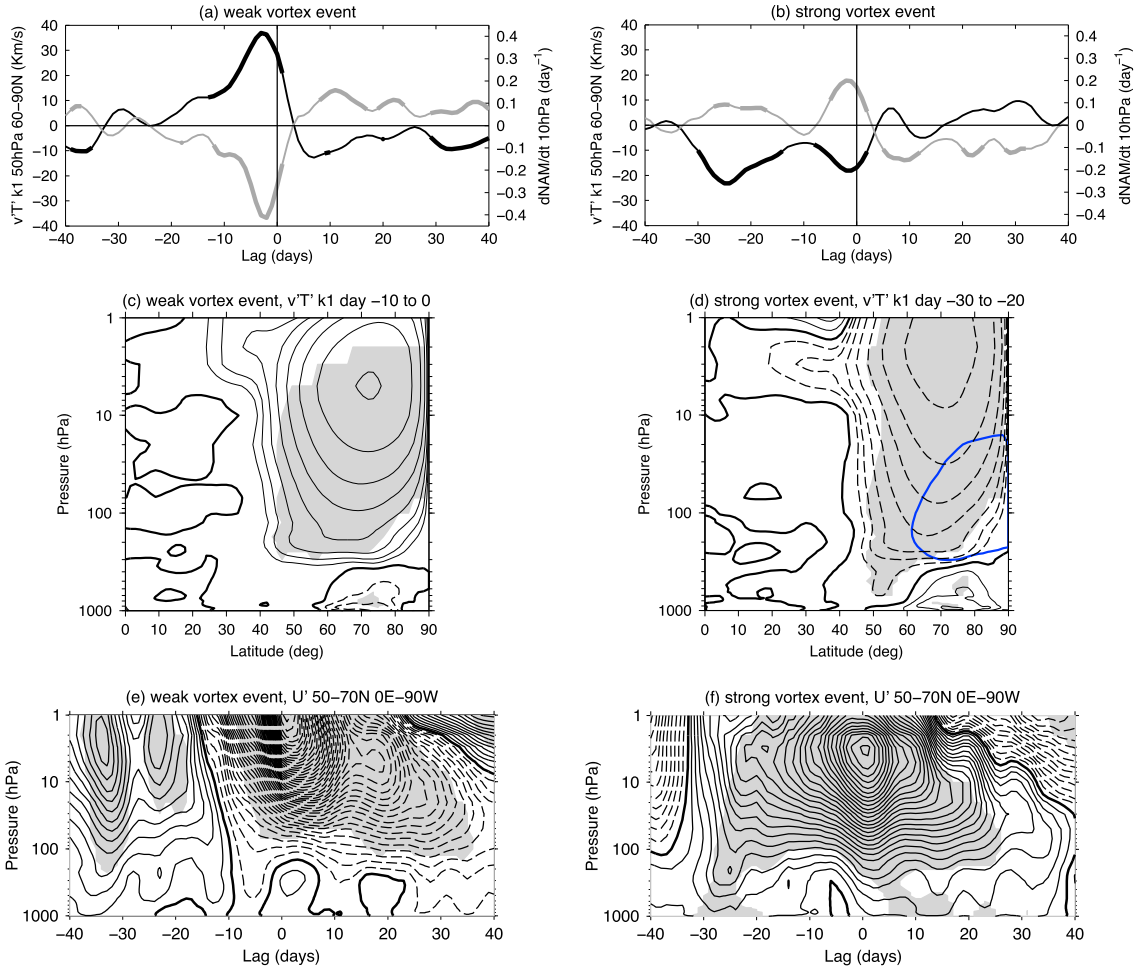

Figure 8. Evolution of the (a, c, e) weak and (b, d, f) strong vortex events from days −40 to +40: (a, b) wave-1 meridional heat flux anomaly at 50 hPa averaged 60 to 90°N (black line) and NAM tendency at 10 hPa (grey line). Statistical significance at the 95% level is denoted with thick lines. (c, d) Wave-1 meridional heat flux anomaly (black contours) and zero contour of the total wave-1 meridional heat flux (blue contour) as a function of latitude and pressure averaged over days −10 to 0 and −30 to −20 for the weak and strong vortex events respectively. Black contour interval is in logarithmic powers of 2: ± [1, 2, 4 ,8, 16, 32, ...] Kms^{-1}. (e, f) Zonal wind anomalies averaged 50 to 70°N and 90°W to 0°E with a contour interval of 1 ms^{-1}. Shading indicates statistical significance at the 95% level. Dashed lines are negative and the thick black line denotes the zero contour for Figures 8c–8f.

We note that the results are consistent with *Shaw et al.* [2014] who showed that stratospheric planetary wave heat flux extremes are instantaneously coupled to N10AO-like circulation anomalies over the North Atlantic.

During the upward wave event, the stratospheric and tropospheric impacts are linked via a deep vertical wave-1 structure as illustrated in the Hovmöller of the 60 – 80°N averaged total wave-1 geopotential height at 10 hPa (shaded contours) and 500 hPa (black contours) in Figure 6a. The 500 hPa wave-1 geopotential height anomalies north of 20°N are shown for lags −10 to −4, −3 to +3 and +4 to +10 days (Figures 6b–6d). The evolution involves a large amplitude quasi-stationary wave-1 pattern in the stratosphere for negative time lags and a westward propagating wave-1 pattern in the troposphere. The evolution involves a clear westward vertical phase tilt with height that transitions to an eastward vertical phase tilt with height around day +5 consistent with the change in sign of the lower stratospheric heat flux during the upward wave event (Figure 2a). The overall pattern of the tropospheric precursor on days −10 to −4 (Figure 6b) is consistent with [*Garfinkel et al.*, 2010] who documented links between negative geopotential height anomalies in the Pacific basin and polar vortex weakening events. The tropospheric patterns on days −10 to −4 and +4 to +10 are consistent with poleward and equatorward North Pacific jet shifts, respectively (not shown). The tropospheric wave-1 signal is westward propagating with an approximate phase speed of −6.3 ms^{-1} from

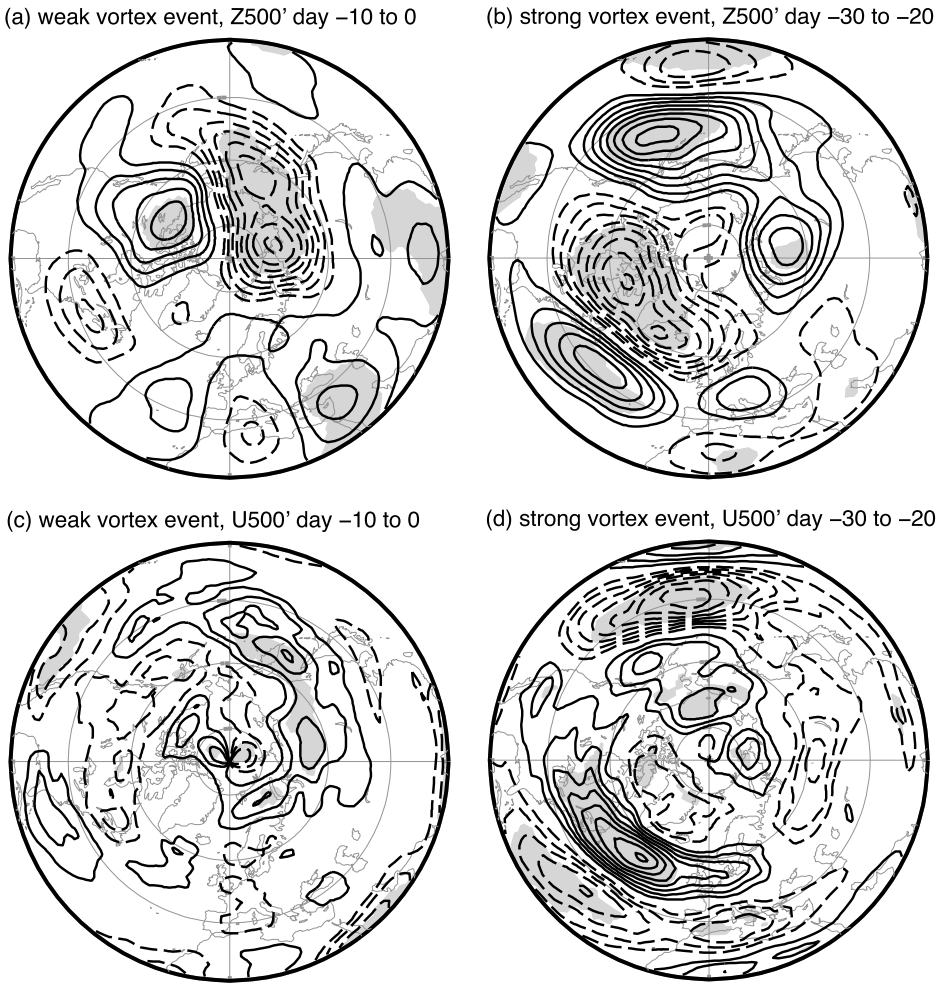

Figure 9. (a, b) Geopotential height anomalies and (c, d) zonal wind anomalies at 500 hPa preceding (a, c) weak and (b, d) strong vortex events averaged over days −10 to 0 and −30 to −20, respectively. Dashed lines are negative and the contour interval is 10 m and 1 ms^{-1} for Figures 9a and 9b and Figures 9c and 9d, respectively. Shading indicates statistical significance at the 95% level based on a two-tailed *t*-test.

days −10 to +10. *Shaw and Perlwitz* [2013] also noted a westward propagating high-latitude wave-1 signal at 500 hPa during their downward wave event (see their Figure 5). The downward wave event exhibits a slower phase speed (−2.6 ms^{-1}) and is 180° out of phase relative to the upward wave event. This opposite phase results in opposite-signed zonal wind anomalies over the North Atlantic during planetary wave events (Figures 5c and 5d).

The results above reveal key features associated with the evolution of planetary wave events. The co-evolution of the stratospheric heat fluxes and the tropospheric anomalies suggests that they have the same dynamical origin. Upward and downward wave events both involve the evolution of a vertically coherent large-amplitude wave-1 structure in high latitudes that couples the stratospheric and tropospheric circulations. In the stratosphere, the wave produces EP flux convergence/divergence resulting in a net deceleration/acceleration during upward/downward wave events. The wave evolution is associated with the evolution of the stratospheric vertical zonal-mean zonal wind shear. In the troposphere, the circulation anomalies are consistent with a westward propagating wave-1 pattern with an opposite longitudinal phase for upward and downward events that produces an equatorward and poleward jet shift in the Atlantic basin, respectively.

A complementary analysis of wave-2 heat flux events is shown in the appendix (Figures A1 and A2). Overall, the evolution of the wave-2 events involve weaker heat flux values and a weaker connection with the NAM

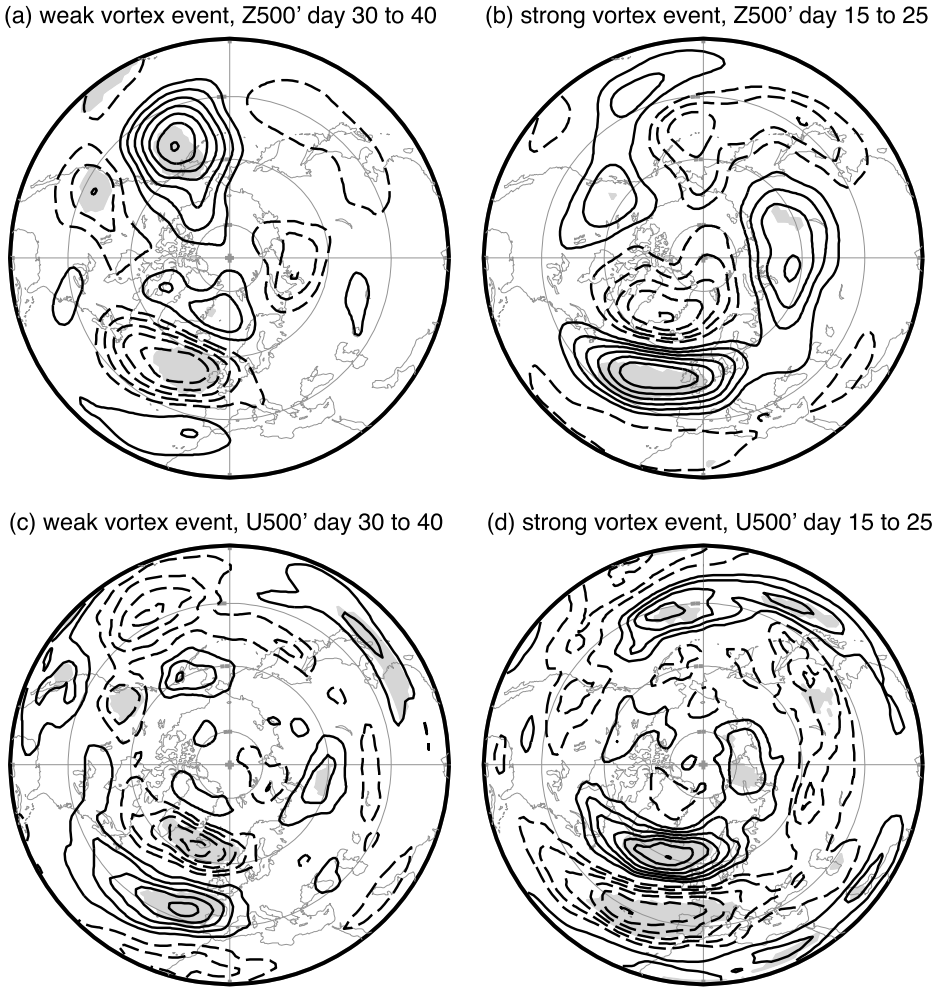

Figure 10. Same as Figure 9, except for (a, c) weak and (b, d) strong vortex events averaged over days +30 to +40 and +15 to +25, respectively.

time-tendency (Figure A2). We note that upward wave-1 and wave-2 events exhibit opposite-signed geopotential height anomalies and an opposite-signed jet shift in the North Atlantic (compare Figures A1 and Figures 5a and 5c). The stratospheric and tropospheric impacts associated with downward wave-2 events are not as robust as the corresponding downward wave-1 events.

3.2. Exploring Connections Between Planetary Wave and Polar Vortex Events

The results in the previous subsection reveal that planetary wave events have a large impact on the time-tendency of the stratospheric zonal-mean flow. In this section, we examine the connection between planetary wave and vortex events on daily time scales to better understand the relationship between them.

We begin by assessing the instantaneous correlation between the two extreme stratospheric event indices. Figure 7a shows the scatter plot of daily NAM index versus the 50 hPa high-latitude total eddy (deviation from the zonal-mean) heat flux during JFM. Blue and red stars/lines denote days when the total eddy heat flux/NAM index are extreme defined based on the percentile of the zero eddy heat flux (e.g., 10th/90th percentiles). The instantaneous correlation between the high-latitude eddy heat flux and NAM index is weak but is larger for negative time lags (Figure 7c, blue dashed), consistent with *Polvani and Waugh* [2004] (see their Figure 3). Similar time-lagged correlations are found between the NAM and the wave-1 heat flux (Figure 7c, blue solid). *Polvani and Waugh* [2004] demonstrated that 40 day time-integrated total eddy heat flux anomalies averaged between 45 and 75°N at 100 hPa are well correlated with the 10 hPa NAM index

(correlation value is ~ -0.75). We find that the correlation value for the same fields in the ERA-Interim data set is −0.7 and is dominated by the wave-1 component (not shown). While there is no significant instantaneous relationship between the eddy heat flux and NAM values, there is a tendency for extreme positive/negative heat flux values to be associated with extreme positive/negative NAM values (see top-left and bottom-right quadrants of Figure 7a).

The high-latitude total eddy heat flux and NAM time-tendency exhibit a significant instantaneous correlation with a value of −0.73 (Figure 7c, black dashed). The wave-1 contribution to the total eddy heat flux dominates the overall correlation (Figure 7c, black solid). The lag correlations between the daily 10 hPa NAM time-tendency and the high-latitude total eddy heat flux are much weaker (Figure 7c, black dashed). The connection between the total eddy heat flux and NAM tendency also holds for the extreme values (Figure 7b) consistent with the results of life cycle analysis (see Figures 4c and 4d). There is a weaker correlation between the high-latitude wave-2 heat flux and the NAM time-tendency (−0.38) in comparison to wave-1 (−0.56), consistent with its smaller contribution to the total eddy heat flux (Figure A2).

The results suggest that the daily eddy and wave-1 heat fluxes are more closely associated with the NAM time-tendency than the value of the NAM itself, as expected from the transformed Eulerian-mean momentum equation. While the relationship is consistent with the well-known connection between positive heat fluxes and weak vortex events via negative NAM tendencies, the results suggest a connection between negative heat fluxes and strong vortex events via positive NAM tendencies. In the next section, we asses the contribution of planetary wave events during the life cycle of vortex events, including their role in the coupling to the tropospheric circulation.

3.3. Comparing and Contrasting the Life Cycles of Planetary Wave and Polar Vortex Events

Here we analyze the composite life cycle of vortex events defined in section 2.3 and listed in Table I. Since the detailed life cycle of vortex events have been documented previously [*Limpasuvan et al.*, 2004, 2005], we focus on (1) assessing the role of wave-1 heat fluxes during vortex events, including their role in the mean flow evolution and coupling to the troposphere, and (2) comparing the patterns and magnitudes of the tropospheric circulation responses in the North Atlantic during vortex events with those during planetary wave events. The results in sections 3.1 and 3.2 suggest that monitoring the magnitude and sign of the lower stratospheric heat flux may shed light on the processes that couple the stratosphere to the troposphere during vortex events.

The evolution of the high-latitude wave-1 heat flux anomaly at 50 hPa and the NAM time-tendency at 10 hPa during weak and strong vortex events is shown in Figure 8. The transient evolution of the vortex events are broadly similar to the planetary wave events but occur on a longer time scale. In particular, the anomalous positive wave-1 heat flux leads to deceleration of the polar vortex whereas anomalous negative wave-1 heat flux leads to acceleration of the polar vortex (compare Figures 8a and 8b and Figures 4c and 4d). While the total wave-1 heat fluxes during vortex events are not in the 5th and 95th percentiles used to define planetary wave events, they nevertheless represent extreme values (22nd and 78th percentile) and their evolution is consistent with the mean flow coupling during planetary wave events. The zonal-mean cross sections of the heat flux anomalies during peak times (−10 to 0 for weak vortex events and −30 to −20 for strong vortex events) are shown in Figures 8c and 8d. The heat flux anomalies exhibit vertical dipoles in high latitudes consistent with the life cycles of planetary wave events (compare Figures 8c and 8d and Figures 2a and 2b). In particular, the total wave-1 heat flux is negative in high latitudes (see blue contour) during the strong vortex event. There is also a rapid reversal of the total wave-1 and wave-2 heat fluxes in high latitudes near day 0 of the strong vortex event (not shown). We note that the reversal of the heat flux prior to the composite strong vortex event is supported by the statistic that all 17 strong vortex events are preceded by 1 or more total negative wave-1 heat flux events within 30 days. During the days of peak heat flux, the high-latitude heat flux patterns coincide with clear vertical dipoles of EPFD coupling the stratosphere and troposphere and are consistent with the sign of the vertical zonal-mean zonal wind shear in high latitudes during the life cycles of planetary wave events (not shown).

The coupling to the tropospheric circulation during vortex events is shown in Figures 8e and 8f. We focus on the Atlantic region and connect the evolution to the high-latitude stratospheric heat flux. Here we use a latitudinal average from 50 to 70°N to better reflect the evolution of the zonal wind anomalies during vortex events. During the weak vortex event, both the wave-1 and wave-2 heat fluxes are large and positive from days −5 to 5. Recall that upward wave-1 and wave-2 events are linked to opposite-signed zonal wind

anomalies over the North Atlantic (see Figures 5 and A1c). This suggests possible cancellation of the tropospheric circulation anomalies driven by the different wave components during this time. Negative Atlantic zonal wind anomalies in the troposphere occur between days +20 to +40 when the heat flux anomalies are weak. During this time, meridional EPF convergence by synoptic waves is important consistent with *Limpasuvan et al.* [2004]. During the strong vortex event, significant positive Atlantic zonal wind anomalies occur during days −30 to −20 and coincide with total negative wave-1 heat fluxes (compare Figures 8d and 8f). Following the event, positive wind anomalies occur in the troposphere from days +5 to +30, and during this time, there is meridional EPF divergence by wave-1 and synoptic-scale waves consistent with *Limpasuvan et al.* [2005].

Finally, we compare the time-averaged tropospheric impacts over the entire Northern Hemisphere during vortex and planetary wave events (Figures 9 and 10). We focus on two periods: (1) the time period of largest stratospheric heat flux and (2) the time period with the strongest tropospheric impacts over the North Atlantic following vortex events. During the strong vortex event, the negative wave-1 heat flux occurs from days −30 to −20. This coincides with clear high-latitude wave-1 geopotential height anomalies that are associated with a poleward North Atlantic jet shift, consistent with the connection between downward wave events and the North Atlantic circulation shown in section 3.1 (compare Figure 9 and Figures 5b and 5d). A similar connection holds around day 0 when the high-latitude wave-1 stratospheric heat flux changes sign (not shown). During the weak vortex event, the maximum wave-1 heat flux occurs from days −10 to 0. This coincides with weak circulation anomalies in the North Atlantic. During this time, both the wave-1 and wave-2 heat fluxes are large and positive in the stratosphere suggesting the weak circulation anomalies are the result of destructive interference between the circulation patterns driven by the different wave components. When the wave-1 heat flux is large and the wave-2 heat flux is small (days −30 to −10), the tropospheric circulation exhibits a clear equatorward jet shift in the North Atlantic consistent with the composite upward wave event (not shown). We note that the patterns of geopotential height anomalies in the north Pacific when the heat flux is largest are consistent with *Garfinkel et al.* [2010] who documented a correlation between geopotential height anomalies in the North Pacific and vortex events.

The largest tropospheric impacts in the North Atlantic following weak and strong vortex events occur on days +30 to +40 and +15 to +25, respectively, and are shown in Figure 10. The circulation anomalies during these times do not display a clear wave-1 structure and are focused in the East Atlantic consistent with the role of synoptic waves during that time. We note some sensitivity in the tropospheric impacts following weak vortex events. Additional analysis reveals that the weak vortex events in our composite involving a reversal of the zonal-mean zonal wind at 60°N and 10 hPa show a stronger equatorward Atlantic jet shift than events that are associated with a reversal at higher levels (not shown). Further research is needed to establish the statistical significance of the differences. Overall the tropospheric circulation anomalies during total negative heat flux and strong vortex events are larger amplitude than during weak vortex events (compare Figure 9d to Figures 10c and 10d). In addition, the tropospheric circulation anomalies during planetary wave events are comparable if not larger amplitude than the impacts following vortex events (compare Figures 10 and 9 with Figure 5). This is true irrespective of the averaging period (e.g., when 11 day averaging is used for all events).

Our results show that planetary wave events occur during vortex events and produce large changes to the stratospheric NAM time-tendency on short time scales that contribute toward the evolution of vortex events. Our results are consistent with the time-averaged relationship between anomalous heat flux values and vortex events shown in *Polvani and Waugh* [2004]. However, we have demonstrated that total negative heat flux/downward wave events play a key role in the formation of strong vortex events showing that strong vortex events represent true dynamical events with significant wave-mean flow interaction.

4. Conclusions and Discussion

4.1. Conclusions

The goal of this study was to compare and contrast extreme stratospheric events related to vertical planetary wave coupling and polar vortex strength in order to better understand the full spectrum of stratosphere-troposphere coupling. The key results of this study are

1. Planetary wave events are characterized by a high-latitude wave-1 structure that directly couples the stratospheric and tropospheric circulations. The events exhibit largely equal but opposite time-integrated impacts: upward/downward wave events produce a deceleration/acceleration of the polar vortex via EPFD and an equatorward/poleward jet shift in the North Atlantic. The impacts are associated with a deep vertical wave mode suggesting the stratosphere and troposphere should not be considered as separate layers as suggested by *Plumb* [2010].
2. Consistent with linear theory [c.f. *McIntyre*, 1982] enhanced positive lower stratospheric vertical zonal wind shear, associated with a strengthened polar vortex focused in high latitudes, precedes positive wave-1 stratospheric heat fluxes. Conversely, negative vertical zonal wind shear in the upper stratosphere precedes total negative wave-1 stratospheric heat fluxes consistent with *Shaw and Perlwitz* [2013].
3. Tropospheric coupling during planetary wave events involves a westward propagating wave-1 signal that is faster for the upward wave event and is 180° out of phase with the downward wave event. The opposite longitudinal phase accounts for the opposite-signed jet shifts in the North Atlantic during planetary wave events.
4. Short time scale planetary wave events contribute toward the development of vortex events. In particular, the total wave-1 stratospheric heat flux is negative preceding strong vortex events which clearly demonstrates that strong vortex events represent true dynamical events involving significant wave-mean flow interaction. This is complementary to the contribution of positive heat flux events to weak vortex events.
5. Tropospheric coupling in the North Atlantic preceding vortex events occurs when the wave-1 heat flux dominates the total eddy heat flux in the stratosphere since interference with upward wave-2 events makes the impacts in the troposphere less clear. During the strong vortex event negative heat fluxes produce a poleward jet shift in the North Atlantic, which is larger amplitude and of a similar sign as the impacts after the event associated with synoptic waves. Overall, the tropospheric impacts in the North Atlantic during planetary wave events are comparable if not larger in magnitude than those following vortex events and the strong vortex events exhibit larger impacts than weak vortex events.

4.2. Discussion

The results provide a unified perspective of stratospheric planetary wave and vortex variability and its coupling to the tropospheric circulation. Planetary wave events occur on short time scales and produce NAM time-tendencies that are important for the development of longer-time scale vortex events. While previous authors have noted connections between the waves and mean flow deceleration [e.g., *Limpasuvan et al.*, 2004, 2005; *McDaniel and Black*, 2005; P. Martineau and S.-W. Son, Onset of circulation anomalies during stratospheric vortex weakening events: The role of planetary-scale waves, submitted to *Journal of Climate*, 2014], we have broadened the connection to encompass negative heat flux and mean flow acceleration events. The results demonstrate that strong vortex events are not dissimilar from weak vortex events in that they are true dynamical events involving significant wave-mean flow interaction. In particular, the reversal of the sign of the heat flux is just as important a dynamical event as the reversal in sign of the zonal-mean zonal wind. This is supported by the fact that state-of-the-art models that do not properly represent extreme negative heat flux events in the stratosphere exhibit a biased North Atlantic geopotential height jet stream position in the troposphere [*Shaw et al.*, 2014].

Isolating the behavior of planetary waves was key to providing insights into wave-mean flow interaction that is important for vortex events. Planetary wave events involve deep vertical wave structures that provide a clear mechanism for coupling the stratospheric and tropospheric circulation, supporting previous idealized modeling studies [*Song and Robinson*, 2004]. The events are focused in high latitudes and represent a key dynamical pathway through which Arctic variability can impact the midlatitude circulation. We did not address the reasons why planetary wave heat fluxes become extreme in high latitudes. Several dynamical mechanisms have been proposed in the literature such as stationary-transient wave interactions, instability, and resonance [*Matsuno*, 1970; *Plumb*, 1981; *McIntyre*, 1982; *Tanaka and Tokinaga*, 2002; *Plumb*, 2010]. A better understanding of the dynamical mechanisms responsible for planetary wave events is the subject of current research using idealized modeling.

Appendix A

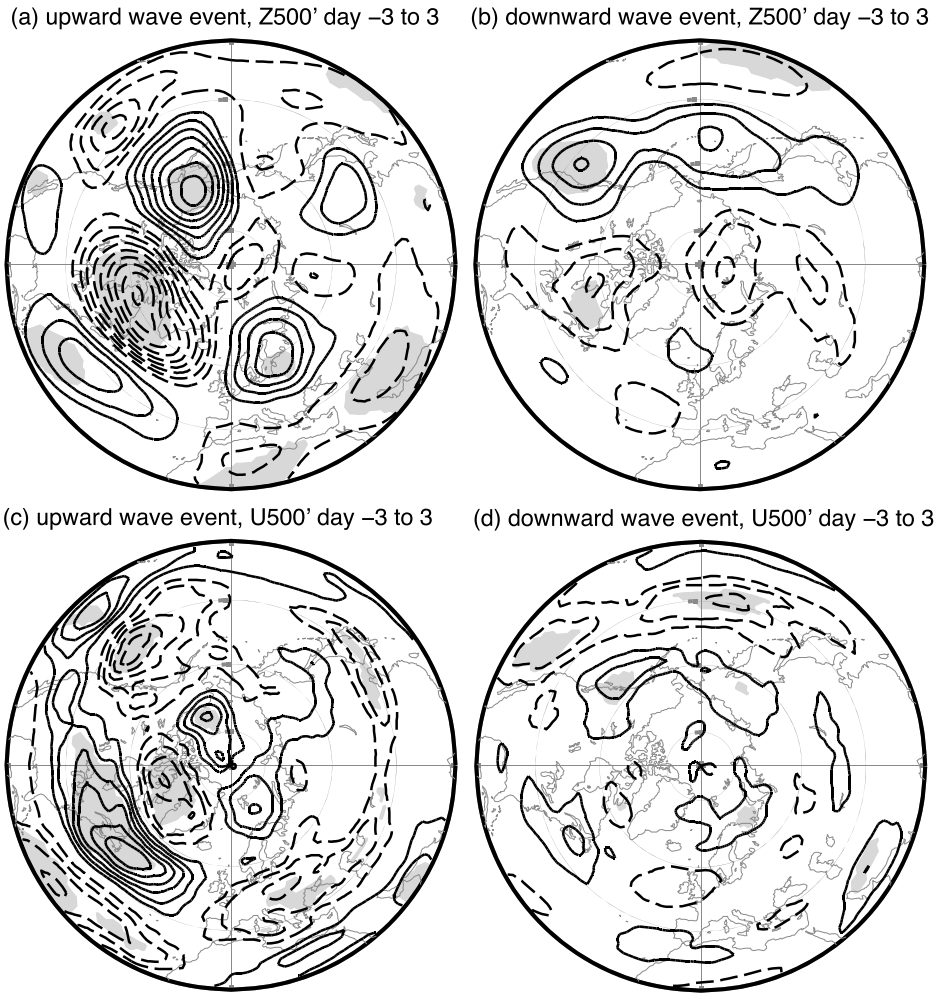

Figure A1. Same as Figure 5, except for (a, c) upward and (b, d) downward wave-2 events.

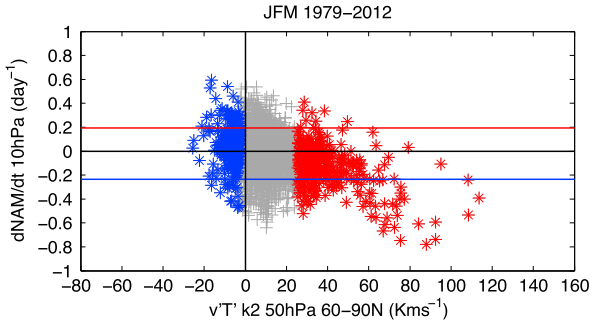

Figure A2. Same as Figure 7b, except for the zonal wave-2 meridional heat flux.

Acknowledgments
E. D. S. and T. A. S. thank J. Perlwitz, I. Simpson, and K. Smith for helpful discussions and comments on the manuscript. E. D. S. and T. A. S. also thank three anonymous reviewers for useful comments and suggestions. T. A. S. also thanks T. Birner for helpful discussions. E. D. S. and T. A. S. are supported by the National Science Foundation under grant AGS-1129519. E. D. S. also acknowledges support from the Natural Sciences and Engineering Research Council of Canada. We thank ECMWF for proving the ERA-Interim data which can be obtained at http://data-portal.ecmwf.int/data/d/interim_daily/.

References

Andrews, D. G., J. R. Holton, and C. B. Leovy (1987), *Middle Atmosphere Dynamics*, 489 pp., Academic, San Diego, Calif.
Baldwin, M. P., and T. J. Dunkerton (2001), Stratospheric harbingers of anomalous weather regimes, *Science*, *294*, 581–584.
Baldwin, M. P., and D. W. J. Thompson (2009), A critical comparison of stratosphere-troposphere coupling indices, *Q. J. R. Meteorol. Soc.*, *97*, 1412–1417.
Charney, J. G., and P. G. Drazin (1961), Propagation of planetary-scale disturbances from the lower into the upper atmosphere, *J. Geophys. Res.*, *66*, 83–109.
Dee, D. P., et al. (2011), The ERA-Interim reanalysis: Configuration and performance of the data assimilation system, *Q. J. R. Meteorol. Soc.*, *137*, 553–597.
Dunkerton, T. J., C. P. F. Hsu, and M. E. McIntyre (1981), Some Eulerian and Lagrangian diagnostics for a model stratospheric warming, *J. Atmos. Sci.*, *38*, 819–844.
Garfinkel, C. I., D. L. Hartmann, and F. Sassi (2010), Tropospheric precursors of anomalous northern Hemisphere stratospheric polar vortices, *J. Clim.*, *23*, 3282–3299.
Gerber, E. P., et al. (2010), Stratosphere-troposphere coupling and annular mode variability in chemistry-climate models, *J. Geophys. Res.*, *115*, D00M06, doi:10.1029/2009JD013770.
Hitchcock, P., T. G. Shepherd, and G. L. Manney (2013), Statistical characterization of arctic polar-night jet oscillation events, *J. Clim.*, *26*, 2096–2116.
Limpasuvan, V., D. W. J. Thompson, and D. L. Hartmann (2004), The life cycle of the Northern Hemisphere sudden stratospheric warmings, *J. Clim.*, *17*, 2584–2596.
Limpasuvan, V., D. L. Hartmann, D. W. J. Thompson, K. Jeev, and Y. L. Yung (2005), Stratosphere-troposphere evolution during polar vortex intensification, *J. Geophys. Res.*, *110*, D24101, doi:10.1029/2005JD006302.
Matsuno, T. (1970), Vertical propagation of stationary planetary waves in the winter Northern Hemisphere, *J. Atmos. Sci.*, *66*, 871–883.
McDaniel, B. A., and R. X. Black (2005), Intraseasonal dynamical evolution of the Northern Annular Mode, *J. Clim.*, *18*, 3820–3839.
McIntyre, M. E. (1982), How well do we understand the dynamics of stratospheric warmings?, *J. Meteorol. Soc. Jpn.*, *60*, 37–65.
McLandress, C., and T. G. Shepherd (2009), Impact of climate change on stratospheric sudden warmings as simulated by the Canadian Middle Atmosphere Model, *J. Clim.*, *22*, 5449–5463.
Newman, P. A., E. R. Nash, and J. E. Rosenfield (2001), What controls the temperature of the arctic stratosphere during the spring?, *J. Geophys. Res.*, *106*, 19,999–20,010.
Palmer, T. N., and C. P. F. Hsu (1983), Stratospheric sudden coolings and the role of nonlinear wave interactions in preconditioning the circumpolar flow, *J. Atmos. Sci.*, *40*, 909–928.
Perlwitz, J., and N. Harnik (2003), Observational evidence of a stratospheric influence on the troposphere by planetary wave reflection, *J. Clim.*, *16*, 3011–3026.
Perlwitz, J., and N. Harnik (2004), Downward coupling between the stratosphere and troposphere: The relative roles of wave and zonal mean processes, *J. Clim.*, *17*, 4902–4909.
Plumb, R. A. (1981), Instability of the distorted polar night vortex: A theory of stratospheric warmings, *J. Atmos. Sci.*, *38*, 2514–2531.
Plumb, R. A. (2010), Planetary waves and the extratropical winter stratosphere, in *The Stratosphere: Dynamics, Transport, and Chemistry, Geophys. Monogr. Ser.*, vol. 190, edited by L. M. Polvani, A. H. Sobel, and D. W. Waugh, pp. 23–41, AGU, Washington, D. C.
Polvani, L. M., and D. W. Waugh (2004), Upward wave activity flux as a precursor to extreme stratospheric events and subsequent anomalous surface weather regimes, *J. Clim.*, *17*, 3548–3554.
Shaw, T. A., and J. Perlwitz (2013), The life cycle of Northern Hemisphere downward wave coupling between the stratosphere and troposphere, *J. Clim.*, *26*, 1745–1763.
Shaw, T. A., and J. Perlwitz (2014), On the control of the residual circulation and stratospheric temperatures in the arctic by planetary wave coupling, *J. Atmos. Sci.*, *71*, 195–206.
Shaw, T. A., J. Perlwitz, and N. Harnik (2010), Downward wave coupling between the stratosphere and troposphere: The importance of meridional wave guiding and comparison with zonal-mean coupling, *J. Clim.*, *23*, 6365–6381.
Shaw, T. A., J. Perlwitz, and O. Weiner (2014), Troposphere-stratosphere coupling: Links to North Atlantic weather and climate, including their representation in CMIP5 models, *J. Geophys. Res. Atmos.*, *119*, 5864–5880, doi:10.1002/2013JD021191.
Song, Y., and W. A. Robinson (2004), Dynamical mechanisms for stratospheric influences on the troposphere, *J. Clim.*, *61*, 1711–1725.
Tanaka, H. L., and H. Tokinaga (2002), Baroclinic instability in high latitudes induced by polar vortex: A connection to the Arctic Oscillation, *J. Atmos. Sci.*, *59*, 69–82.

Erratum

In the originally published version of this article, an error was found in the calculation of planetary wave event calendar dates. The error extended to Figures 1–7, Figures A1 and A2, Table 1, and data described in reference to these figures and table. The figures and table have been replaced and the text has since been corrected. This version may be considered the authoritative version of record.